Influence of Mn doping on $CuGaS_2$ single crystals grown by CVT method and their characterization

2008 J. Phys. D: Appl. Phys. 41 115102

(http://iopscience.iop.org/0022-3727/41/11/115102)

IOP PUBLISHING JOURNAL OF PHYSICS D: APPLIED PHYSICS

J. Phys. D: Appl. Phys. **41** (2008) 115102 (6pp) doi:10.1088/0022-3727/41/11/115102

Influence of Mn doping on $CuGaS_2$ single crystals grown by CVT method and their characterization

P Prabukanthan and R Dhanasekaran[1]

Crystal Growth Centre, Anna University, Chennai–600 025, India

E-mail: rdhanasekaran@annauniv.edu

Received 6 November 2007, in final form 29 February 2008
Published 9 May 2008
Online at stacks.iop.org/JPhysD/41/115102

Abstract

1 and 2 mole% of Mn doped $CuGaS_2$ (CGS) single crystals were grown by the chemical vapour transport (CVT) technique using iodine as the transporting agent. The analysis of the single crystal x-ray diffraction data suggests that the doping of 1 and 2 mole% Mn in the CGS single crystal does not affect the tetragonal (chalcopyrite) crystal structure. The optical absorption spectrum shows that the Mn ion induces a very strong absorption band in the UV–visible–near IR regions. The values of the crystal parameter (D_q) and the Racah parameter (B) calculated from the absorption spectra show d electron delocalization in the host crystal CGS. Room temperature photoluminescence spectra of undoped CGS only exhibited a band–band emission. But 1 and 2 mole% Mn doped CGS single crystals show two distinct CGS and Mn^{2+} related emissions, both of which are excited via the CGS host lattice. Raman spectra of 1 and 2 mole% Mn doped CGS single crystals exhibit a high intensity peak of the A_1 mode at 310 cm^{-1} and 300 cm^{-1}, respectively. EDAX, optical absorption and Raman spectrum studies reveal that Mn^{2+} ions are substituted in the Ga^{3+} ions and incorporated into the CGS lattice. The magnetization of Mn doped CGS single crystals was measured as a function of the magnetic field and temperature. Paramagnetic behaviour typical of spin $S = 5/2$ expected for Mn^{2+} (d^5) magnetic centres was observed in the temperature range $2\,K < T < 300\,K$. In Mn doping, the increase in bulk conductivity of the Mn doped CGS single crystals at room temperature indicates an increase in the hole concentration.

1. Introduction

Spintronics is the correlation between the charge and spin of the electrons, where it is not only the electron charge but also the electron spin that carries information, and this offers opportunities for a new generation of devices. In comparison with conventional semiconductor devices, spintronic devices are promising in improving data processing speed, reducing electric power consumption and increasing integration densities [1, 2]. Due to the great advantages in possible electronic devices, intensive attention has been paid to semiconductor based ferromagnetic (FM) materials, including Mn doped III–V [3,4] and chalcopyrite [5,6] semiconductors. Mn doped ternary I–III–VI_2 compounds, which crystallize in the chalcopyrite type structure (space group $I\bar{4}2d$), were proposed as a new class of FM semiconductors [7]. In the $CuGaS_2$ (CGS) semiconductor, the impurities (Mn) tend to enter substitutionally into the metal sublattice. This is partly due to the flexibility in structure and the fact that two different cation sites exist in this crystal. The energy for Mn substitution in Ga (0.43 eV Mn^{-1}) is lower than that for the Cu site (0.80 eV Mn^{-1}) [8]. This implies that Mn substitutes on the Ga site rather than on the Cu site [2, 8]. By *ab initio* calculations [8] it was found that the FM state is strongly favoured with the Curie temperature of 160 K in $CuGaS_2$ materials substituted with Mn on the Ga site. The ferromagnetism (considering the Mn pair as first neighbour) decreases in the sequence $CuAlS_2 \rightarrow CuGaS_2 \rightarrow CuInS_2$ and $CuGaS_2 \rightarrow CuGaSe_2 \rightarrow CuGaTe_2$, i.e. the FM stability becomes weaker when the cation or the anion becomes heavier in these chalcopyrites [2]. Besides theoretical calculations only a few experimental results concerning the

[1] Author to whom any correspondence should be addressed.

Table 1. Single crystal XRD lattice parameters, volume of unit cell, tetragonal distortion (δ), anion displacement (w) and composition of as-grown undoped and 1 and 2 mole% Mn doped $CuGaS_2$ single crystals.

Samples	Single crystal XRD data			δ	w	Atomic % of elements (stoichiometry value)			
	a (Å) (±0.0002)	c (Å) (±0.0002)	Volume of unit cell (Å^3) (±0.1)			Cu	Ga	S	Mn
Undoped $CuGaS_2$	5.2496	10.4493	300.4	0.0095	0.4387	24.86 (25)	24.92 (25)	50.22 (50)	—
1 mole% Mn doped $CuGaS_2$	5.2504	10.4502	300.2	0.0096	0.4387	24.93 (25)	23.98 (25)	50.20 (50)	0.89
2 mole% Mn doped $CuGaS_2$	5.2512	10.4509	300.2	0.0098	0.4387	24.98 (25)	23.06 (25)	50.17 (50)	1.79

I–III–VI_2 chalcopyrite with Mn substitution can be found in the literature. Lin *et al* [9] studied $Cu_{1-x}Mn_xInTe_2$ and reported paramagnetic behaviour ($x = 0.03$) and antiferromagnetic coupling ($0.09 < x < 0.12$) and this material ($0.03 < x < 0.09$) shows an anomalous magnetic behaviour at low temperature. Tsujii *et al* [10] reported the absence of magnetic ordering in $CuB_{1-x}Mn_xS_2$ (B = In and Fe) down to 2 K, concluding that short-range antiferromagnetic interactions are dominating and the interaction via carrier electrons or holes is not important. In CGS, substitution of Mn^{2+} on the Ga site produces holes but the substitution on the monovalent Cu site is expected to produce electrons and hence no ferromagnetism [2]. Freeman and Zhao [11] have reported that a new class of half-metallic FM semiconductors in Mn doped I–III–VI_2 chalcopyrites is predicted with the Curie temperature proportional to the hole concentration. Novotortsev *et al* [12] studied $CuGaTe_2\langle Mn\rangle$ and reported Mn^{2+} ions containing Mn on one or two cation sites and superparamagnetic clusters. Sato *et al* [13] studied the 5 mole% Mn doped CGS single crystal having no photoluminescence (PL) and no fine structures can be observed below the absorption edge. Mn can be incorporated into the chalcopyrite of the CGS lattice by suitably adjusting the growth parameters.

2. Experimental procedure

The growth and characterization of pure $CuGaS_2$ (CGS) single crystals have been reported earlier [14]. The Mn impurity was added during crystal growth. Single crystals of CGS were grown by chemical vapour transport (CVT) in a closed quartz ampoule using iodine as a transporting agent with an amount of 1 or 2 mole% of Mn. Stoichiometric compositions of constituent elements with a total weight of 1 g were taken in the ampoule with iodine of 10 mg cm^{-3} and the closed ampoule was placed in a two-zone horizontal electrical furnace. The source and growth zone temperatures were 1173 K and 1023 K, respectively. The growth period was 7 days. The furnace was slowly cooled at a rate of 10 K h^{-1} up to 873 K; after reaching this temperature it was cooled rapidly at a rate of 60 K h^{-1}. The crystals grown with 1 and 2 mole % Mn doped CGS single crystals were green and orange in colour with dimensions of $2.5 \times 3 \times 4$ mm^3 and $4 \times 3 \times 3$ mm^3, respectively.

As-grown Mn doped CGS crystals were studied by single crystal XRD, powder x-ray diffraction, energy dispersive x-ray analyser (EDAX), PL, Raman and electrical studies. The details of the equipment used to study the grown crystals have been given earlier [14]. Magnetic measurements (M–H and M–T) have been carried out using the commercial Quantum Design superconducting quantum interference device (SQUID) magnetometer.

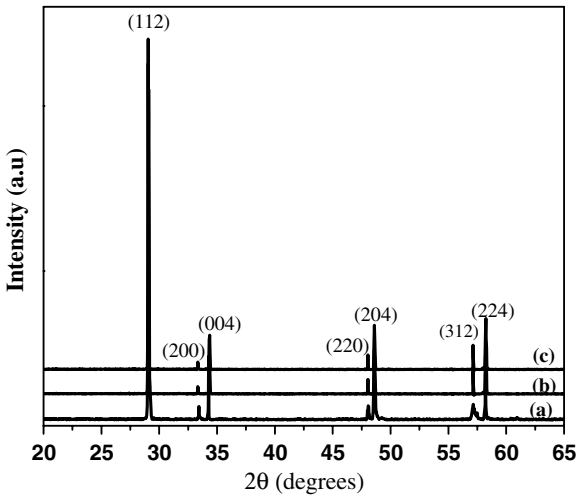

Figure 1. Powder XRD spectra of (a) undoped CGS crystal, (b) 1 mole% Mn doped CGS crystal and (c) 2 mole% Mn doped CGS crystal.

3. Results and discussion

The single crystal x-ray diffraction analysis shows that the as-grown undoped and 1 and 2 mole% Mn doped $CuGaS_2$ (CGS) single crystals have a tetragonal (chalcopyrite) system and the space group is $I\bar{4}2d$. The lattice constants and the volume of a unit cell of undoped and 1 and 2 mole% Mn doped CGS single crystals were obtained and are reported in table 1. Figures 1(a), (b) and (c) show the powder XRD patterns for the undoped and 1 and 2 mole% Mn doped CGS crystals, respectively. The powder XRD patterns of Mn doped CGS show no additional peaks due to the formation of any secondary phases such as MnS, Cu_2S and Ga_2S_3 or Mn alloy. The following crystallographic parameters for undoped and Mn doped CGS crystals have been calculated: tetragonal distortion [$\delta = 2 - (c/a)$] and anion displacements $(c/a)^2 = 2 + 32(1/2 - w)$. The values of δ and w are presented in table 1. The doping of CGS single crystals with Mn has no effect on δ and w, which implies that Mn substitution does not change the symmetry of the CGS structure, which remains close to that of the chalcopyrite structure.

The composition analysis of as-grown undoped and Mn doped CGS single crystals was carried out using EDAX. The results of the corresponding elements in atomic percentage are

given in table 1. From table 1, it can be observed that there is deviation in the compositions of Ga, when the concentration of Mn increases in CGS single crystals. The results indicate that Mn might act as a substitute at the Ga site in the CGS single crystal system.

Absorption coefficients (α) were estimated from the absorption spectra recorded for undoped and 1 and 2 mole% Mn doped CGS single crystals. Figure 2 shows the value of $(\alpha h\nu)^2$ versus the photon energy. It is observed that in 1 mole% Mn doped CGS single crystals, there are five absorption bands with energies of 1.45, 1.65, 1.82, 2.06 and 2.33 eV in the absorption region which correspond to the transitions $^6A_1(^6S) \rightarrow {}^4T_1(^4G)$, $^6A_1(^6S) \rightarrow {}^4T_2(^4G)$, $^6A_1(^6S) \rightarrow {}^4E_1$, $^4A_1(^4G)$, $^6A_1(^6S) \rightarrow {}^4T_2(^4D)$ and $^6A_1(^6S) \rightarrow {}^4E_4(^4D)$ of the Mn^{+2} ion in the cubic (T_d) crystal field. The absorption band (1 mole%) with the energy at 2.36 eV is near the band gap of the CGS host lattice. In the case of 2 mole% Mn doped CGS single crystals, the intensity of absorption band transitions is very low and the absorption band energies (1.15, 1.25, 1.37, 1.50 and 1.64 eV) are also shifted towards the lower band gap when compared with the 1 mole% Mn doped CGS single crystals. The absorption band (2 mole%) with the energy at 1.95 eV is near the band gap of the CGS host lattice. The exact mechanism of the shift in the absorption bands and the lower intensity is not yet clearly understood. The 1 mole% Mn doped $CuGaS_2$ single crystals were found with a higher intensity compared with that of 2 mole% Mn doped $CuGaS_2$ single crystals. It is reported in the literature that no fine structure is observed below the absorption edge [13] in the case of 5 mole% Mn doped CGS single crystals. The parameters of the Mn^{2+} ion in CGS single crystals, such as the crystal field parameter (D_q) and the Racah parameter (B), deduced from the absorption spectra, are listed in table 2. The values of Mn doped CGS single crystals are very close to those of Mn^{2+} in ZnS for which the values D_q and B are 545 and 500 cm^{-1}, respectively [15]. Crystal field theory is based on the assumption of pure electrostatic forces, i.e. polar bonds. The crystal field parameter (D_q) value of Mn doped CGS single crystal is high when compared with that of Mn doped ZnS. In the chalcopyrite structure of CGS, each Cu or Ga has four anions of S as nearest neighbours and each S anion has two Cu and two Ga cations as its nearest neighbours. The Ga–S and Cu–S bond lengths are unequal [16]. The S atoms in ZnS have regular tetrahedral coordination and the Zn–S bond length is close to the Ga–S bond length in CGS. Mn substitution on the Cu site creates longer bonds than the host Cu–S bond, indicating that the Mn tetrahedral radius is larger than that of Cu. But due to the substitution of Mn on the Ga site, the bond is unchanged, suggesting a similar tetrahedral radius for Ga and Mn [2]. The above consideration of the crystal field and the electronegativity difference between the atoms may indicate that Mn atoms are substituted in the Ga sites.

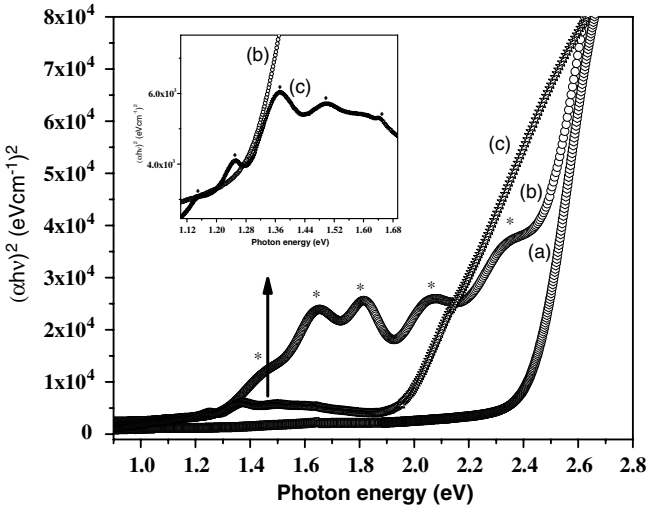

Figure 2. $(\alpha h\nu)^2$ versus photon energy of as-grown (a) undoped $CuGaS_2$ single crystal, (b) 1 mole% Mn doped $CuGaS_2$ single crystal and (c) 2 mole% Mn doped $CuGaS_2$ single crystal recorded at room temperature. The inset shows the corresponding enlarged optical spectra for the 2 mole% Mn doped $CuGaS_2$ single crystal.

Figures 1(a), (b) and (c) show the PL emission spectra of undoped and 1 and 2 mole% Mn doped CGS single crystals recorded at room temperature. The measurement conditions were identical in all cases and therefore relative intensities can

Table 2. Spectral positions of the absorption bands, transition, crystal field parameter (D_q) and Racah parameter (B) of Mn^{2+} ions in $CuGaS_2$ single crystals.

Samples	Energy (eV)	Transition	D_q (cm^{-1})	B (cm^{-1})	References
1 mole% Mn doped $CuGaS_2$ single crystals	1.45	$^6A_1(^6S) \rightarrow {}^4T_1(^4G)$	579	535	This work
	1.65	$^6A_1(^6S) \rightarrow {}^4T_2(^4G)$			
	1.82	$^6A_1(^6S) \rightarrow {}^4E_1, {}^4A_1(^4G)$,			
	2.06	$^6A_1(^6S) \rightarrow {}^4T_2(^4D)$			
	2.33	$^6A_1(^6S) \rightarrow {}^4E_4(^4D)$			
2 mole% Mn doped $CuGaS_2$ single crystals	1.15	$^6A_1(^6S) \rightarrow {}^4T_1(^4G)$	543	496	This work
	1.25	$^6A_1(^6S) \rightarrow {}^4T_2(^4G)$			
	1.37	$^6A_1(^6S) \rightarrow {}^4E_1, {}^4A_1(^4G)$,			
	1.50	$^6A_1(^6S) \rightarrow {}^4T_2(^4D)$			
	1.64	$^6A_1(^6S) \rightarrow {}^4E_4(^4D)$			
5 mole% Mn doped $CuAlS_2$ single crystals	2.21	$^6A_1 \rightarrow {}^4T_1$	578	335	[13]
	2.38	$^6A_1 \rightarrow {}^4T_2$			
	2.59	$^6A_1 \rightarrow {}^4E_1, {}^4A_1$			
	2.79	$^6A_1 \rightarrow {}^4T_2$			

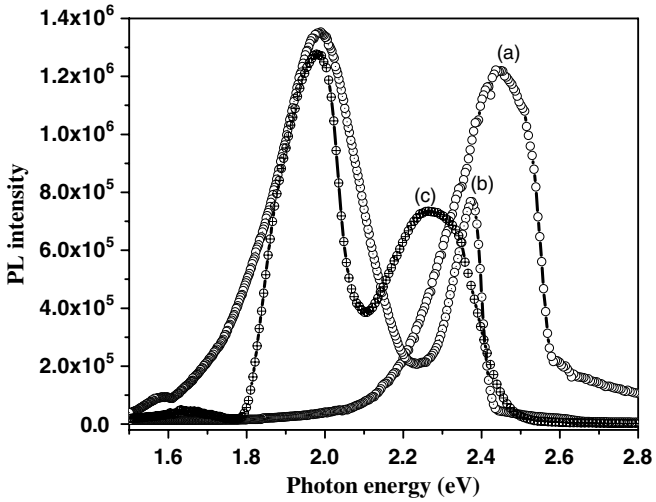

Figure 3. Room temperature PL spectra of as-grown (a) undoped $CuGaS_2$ single crystal, (b) 1 mole% Mn doped $CuGaS_2$ single crystal and (c) 2 mole% Mn doped $CuGaS_2$ single crystal.

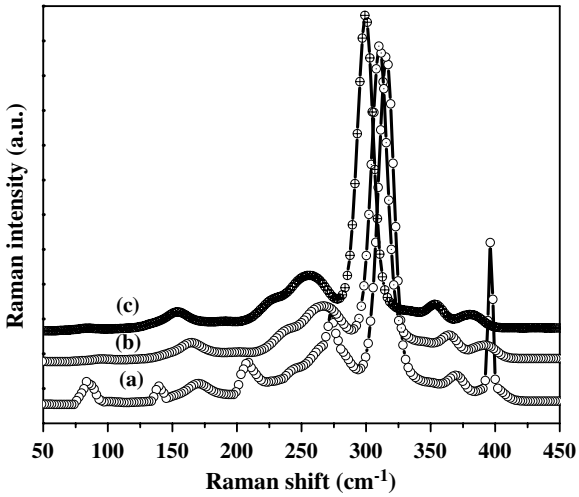

Figure 4. Room temperature Raman spectra of as-grown (a) undoped $CuGaS_2$ single crystal, (b) 1 mole% Mn doped $CuGaS_2$ single crystal and (c) 2 mole% Mn doped $CuGaS_2$ single crystal.

be compared. The PL spectra for the undoped CGS single crystals showed that the strong emission band at 2.446 eV is attributed to the band–band gap luminescence. Two PL emission lines are observed for 1 and 2 mole% Mn doped CGS single crystals. The high intensity PL emission lines are at the same position for the 1 and 2 mole % Mn doped CGS single crystals. The high intensity PL emission line centred at 1.98 eV is attributed to the $^4E_4 \rightarrow {}^6A_1$ transition in the Mn^{2+} ions. The electron from the ground state of Mn^{2+} ($^6A_1$) is excited to the conduction band of CGS by photons. The process may be explained as $Mn^{2+} + h\nu \rightarrow Mn^{3+} + e^-$, where $h\nu$ is the energy needed to cause the photoexcitation of Mn^{2+} in CGS. The free electrons in the conduction band can relax to the $^4E_4$ excited state by a nonradiative process followed by radiative transition from the excited state $^4E_4$ to the $^6A_1$ ground state emitting a strong orange light. The low intensity PL emission lines are at different positions for the 1 and 2 mole% Mn doped CGS single crystals (2.38 and 2.27 eV). However, the 2 mole% Mn doped CGS single crystals have a slightly broader emission when compared with that of 1 mole% Mn doped CGS that also shifts towards a lower band gap (red shift). This peak position and intensity difference may be assigned to the presence of point defects found between the valance band and the conduction band such as recombination from the conduction band to a cation vacancy or the recombination between Mn related acceptor centres. When the Mn concentration is increased the creation of defect energy levels below the conduction band is high. So different peak positions and intensity differences in the PL spectra of as-grown Mn doped $CuGaS_2$ single crystals are observed.

Figures 4(a), (b) and (c) show the Raman spectra of undoped and 1 and 2 mole% Mn doped CGS single crystals. The high intensity peak in the chalcopyrite structure is the symmetric A_1 mode, which in the 1 and 2 mole% Mn doped CGS appeared at 310 and 300 cm^{-1}. The single A_1 mode is observed at 315 cm^{-1} in the pure CGS single crystal [14]. The A_1 mode phonon is purely due to the vibration of S atoms in the *c*-plane with Cu and Ga atoms remaining at rest [17]. In the case of Mn doped CGS single crystals, the A_1 mode shifts towards a lower frequency. It may be due to the existence of the mass effect and the electronegativity difference effect. The electronegativity difference in the Mn–S bond is smaller than that of the Ga–S bond while being larger than that of the Cu–S bond [2, 18]. The mass effect of the stationary atom may be neglected and only the electronegativity difference effect may contribute to Raman shifts. As the Mn^{2+} ions replace the Ga atoms, the energy of the A_1 mode must decrease, since the restoring force of the Mn–S bond is weaker than that of the Ga–S bond.

The magnetic properties of 1 and 2 mole% Mn doped CGS single crystals have been investigated using a SQUID magnetometer. The temperature dependence of magnetization (M–T) measured in the magnetic field of 250 Oe is shown in figures 5(*a*)–(*b*). The figures show the magnetization measurements of zero field cooled (ZFC) and field cooled (FC) conditions on the materials by applying a field of 250 Oe. It is observed that there is no splitting between ZFC and FC magnetizations measured at 250 Oe. The samples show paramagnetic behaviour following the Curie–Weiss law. Considering inverted magnetization at different temperatures, a Curie–Weiss behaviour $\chi = C/T + \Theta$ at Curie–Weiss temperatures of $\Theta = -20$ and -38 K can be observed in 1 and 2 mole% Mn doped CGS single crystals. This implies that magnetic Mn^{2+} ions in the lattice are coupled antiferromagnetically (AFM). The effective magnetic moment (μ_{eff}) calculated from this curve is 5.18 and 5.23 μ_B per Mn atom in 1 and 2 mole% Mn doped CGS single crystals. It is also reported that the samples with 3% Mn in $Cu_{1-x}Mn_xInTe_2$ ingots are paramagnetic [9]. It implies that the sample is paramagnetic and no FM contribution has been detected. Figures 6(*a*)–(*b*) show the magnetic field versus magnetization for Mn doped CGS single crystals. No hysteresis loops were observed at 2, 15 and 30 K for the 1 and 2 mole% Mn doped CGS single crystals. The curves are composed of diamagnetic and paramagnetic components.

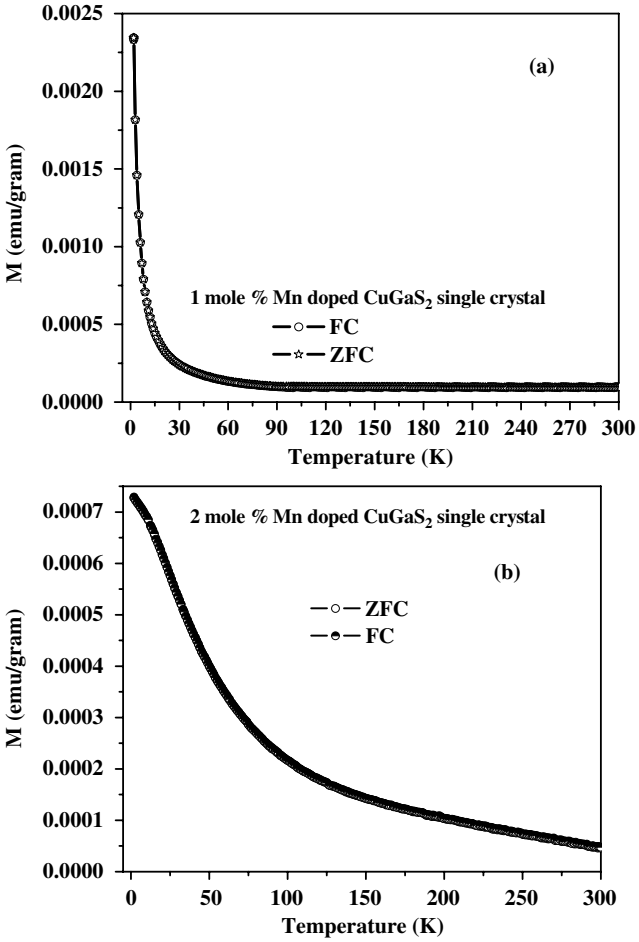

Figure 5. Magnetization versus temperature (M–T) curves of (a) 1 mole% Mn doped $CuGaS_2$ single crystal and (b) 2 mole% Mn doped $CuGaS_2$ single crystal. The measurement was performed in the two processes of field cooling (FC) and zero field cooling (ZFC), with a magnetic field of 250 Oe applied perpendicular to the single crystals.

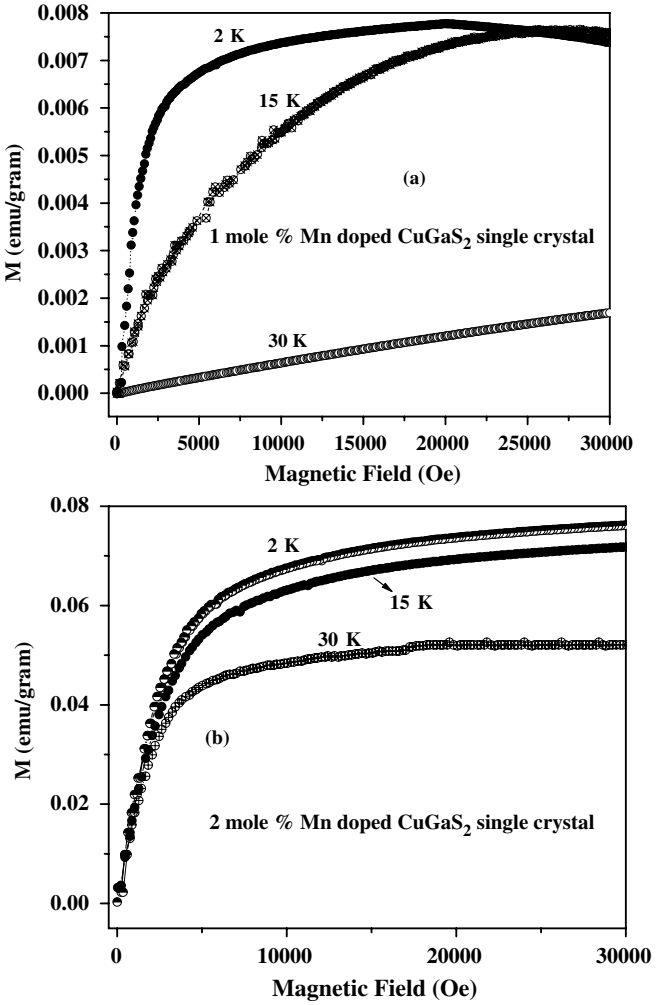

Figure 6. Magnetization versus magnetic field (M–H) curves of (a) 1 mole% Mn doped $CuGaS_2$ single crystal and (b) 2 mole% Mn doped $CuGaS_2$ single crystal at different temperatures of 2, 15 and 30 K.

The Heisenberg model to estimate the Curie temperature [T_C] in ordered $CuMn_xGa_{1-x}S_2$ ($x = 0.5$ and 0.25) alloys gives $T_C \sim 180$ K and 176 K [8], respectively. In our case, 1 and 2 mole% Mn doped $CuGaS_2$ single crystals have a low Mn concentration; the compositions of Mn in $CuGaS_2$ are $x = 0.0356$ and $x = 0.0716$, respectively, estimated from EDAX. The SQUID measurements confirm that it was a paramagnetic material.

The electrical measurements of 1 and 2 mole% Mn doped CGS single crystals were carried out using the Hall effect apparatus with the van der Pauw configuration at room temperature. In table 3, the results of the electrical characterization of undoped and 1 and 2 mole% Mn doped CGS single crystals at room temperature are listed. The 1 and 2 mole% Mn doped CGS single crystals have higher hole mobility and hole concentration and the resistivity decreases when compared with undoped CGS. These results are indicative of a high degree of ionized impurity scattering at room temperature due to the presence of Mn which can be tentatively explained by assuming that Mn acts as an acceptor in this material. The Mn doped CGS single crystals have p-type conductivity.

4. Conclusion

Single crystals of undoped and 1 and 2 mole% Mn doped $CuGaS_2$ (CGS) have been grown by the chemical vapour transport method using iodine as the transporting agent. The x-ray diffraction analysis clearly shows that the Mn doped CGS single crystals are single phase in the chalcopyrite structure. The fundamental absorption edge of the as-grown Mn doped CGS single crystal shows a large change due to Mn^{2+} ions incorporated into the CGS lattice. The optical band-gap energies of Mn doped CGS single crystals decreased as the concentration of the Mn^{2+} ions increased. The observed bands in the optical study have been attributed to transitions from the $^6A_1$ (^6S) ground state to different excited quartet levels of Mn^{2+} ions. The PL spectrum of 1 and 2 mole% Mn doped CGS single crystals has emission peaks at 2.38 and 1.98 eV and 2.27 and 1.98 eV. In 1 and 2 mole% Mn doped CGS single crystals, the dominant Raman scattering vibration has been attributed to the A_1 mode at 310 and 300 cm^{-1}. The Mn doped CGS single crystals showed paramagnetic behaviour following the Curie–Weiss law. The Curie–Weiss temperature (Θ) was negative for

Table 3. Values of mobility, hole concentration and resistivity of as-grown undoped and 1 and 2 mole% Mn doped $CuGaS_2$ single crystals measured at room temperature.

Sample	Hole mobility ($cm^2\ V^{-1}\ s^{-1}$)	Hole concentration (cm^{-3})	Resistivity (Ω cm)	References
Undoped $CuGaS_2$	17.34	3×10^{17}	1.2	[14]
1 mole% Mn doped $CuGaS_2$	54.32	1.7×10^{18}	0.07	This work
2 mole% Mn doped $CuGaS_2$	77.63	8.29×10^{18}	0.0097	This work

1 and 2 mole% Mn doped CGS single crystals. The calculated values of μ_{eff} for 1 and 2 mole% Mn doped CGS single crystals were 5.18 μ_B and 5.23 μ_B, respectively. Although the hole concentration was successfully increased, no FM nature was observed. It is concluded that the hole concentration induced FM model does not explain our experimental observations. Electron paramagnetic resonance should be an interesting subject for a detailed investigation in future.

Acknowledgments

PP is grateful to the Council of Scientific and Industrial Research [CSIR], India, for the award of a Senior Research Fellowship [SRF].

References

[1] Dietl T, Ohno H, Matsukura F, Cibert J and Ferrand D 2000 *Science* **287** 1019
[2] Zhao Y-J and Zunger A 2004 *Phys. Rev.* B **69** 104422
[3] Ferrand D *et al* 2001 *Phys. Rev.* B **63** 085201
[4] Overberg E M, Gila B P, Abernathy C R, Pearton S J, Theodoropoulou N A, McCarthy K T, Amason S B and Hebard A F 2001 *Appl. Phys. Lett.* **79** 3128
[5] Mevedkia G A, Ishibashi T, Nishi T, Hayata K, Hasequawa Y and Sato K 2000 *Japan. J. Appl. Phys.* **39** L949
[6] Zhao Y-J, Picozzi S, Contineaza A, Geng W T and Freeman A J 2002 *Phys. Rev.* B **65** 094415
[7] Zhao Y-J and Freeman A J 2002 *J. Magn. Magn. Mater.* **246** 145
[8] Picozzi S, ZhaoY-J, Freeman A J and Delley B 2002 *Phys. Rev.* B **66** 205206
[9] Lin L J, Wernick J H, Tabatabaie N, Hull G W and Meagher B 1987 *Appl. Phys. Lett.* **51** 2051
[10] Tsujii N, Kitazawa H and Kido G 2002 *Phys. Status Solidi* a **189** 951
[11] Freeman A J and ZhaoY-J 2003 *J. Phys. Chem. Solids* **64** 1453
[12] Novotortsev V M, Shabunina G G, Koroleva L I, Aminov T G, Demin R V and Boichuk S V 2007 *Inorg. Mater.* **43** 12
[13] Sato K, Morita M, Okamoto S, Morita S, Kambara T, Gondaira K I and Takenoshita H 1984 *Prog. Cryst. Growth Charact.* **10** 311
[14] Prabukanthan P and Dhanasekaran R 2007 *Cryst. Growth Des.* **7** 618
[15] McClure D S 1963 *J. Chem. Phys.* **39** 2850
[16] Jaffe J E and Zunger A 1984 *Phys. Rev.* B **29** 1882
[17] van der Ziel J P, Meixner A E, Kasper H M and Ditzenberger J A 1974 *Phys. Rev.* B **9** 4286
[18] Burns G 1985 *Solid State Physics* (New York: Academic)